European Journal of Pharmaceutics and Biopharmaceutics 80 (2012) 113–121

Contents lists available at SciVerse ScienceDirect

European Journal of Pharmaceutics and Biopharmaceutics

journal homepage: www.elsevier.com/locate/ejpb

Research paper

Fabrication of quercetin nanocrystals: Comparison of different methods

Mitali Kakran [a], Ranjita Shegokar [b], Nanda Gopal Sahoo [a], Loaye Al Shaal [b], Lin Li [a,*], Rainer H. Müller [b]

[a] School of Mechanical and Aerospace Engineering, Nanyang Technological University, Singapore, Singapore
[b] Department of Pharmaceutics, Biopharmaceutics and NutriCosmetics, Institute of Pharmacy, Freie Universität Berlin, Berlin, Germany

ARTICLE INFO

Article history:
Received 20 June 2011
Accepted in revised form 22 August 2011
Available online 28 August 2011

Keywords:
Quercetin
Nanosuspension
High-pressure homogenization
Bead mill
Cavi-precipitation
Saturation solubility

ABSTRACT

The main aim of this study was to prepare quercetin nanocrystals using three fabrication methods, viz. high-pressure homogenization, bead milling, and cavi-precipitation. The three fabrication methods were compared in terms of particle size, saturation solubility, and dissolution of the products obtained. The average particle size of the coarse quercetin was 50.1 μm. The three methods produced quercetin particles in the nanometre range (276–787 nm) and the smallest nanocrystals of around 276.7 nm were fabricated by bead milling. The particle size, polydispersity index, zeta potential, and saturation solubility values for the products fabricated by both high-pressure homogenization and bead mill were similar and thus both represented an efficient means to fabricate quercetin nanosuspensions. According to X-ray diffraction analysis, all nanocrystals were still in the crystalline state after being fabricated by the three methods. The cavi-precipitated product exhibited larger particle size and did not show an optimum stability as suggested by the zeta potential values. However, cavi-precipitated quercetin nanosuspension showed the higher saturation solubility due to the presence of ethanol. The bead milled products with the lowest particle size exhibited a saturation solubility of 25.59 ± 1.11 μg/ml, approximately nine times higher than coarse quercetin. Overall, the dissolution rates of the quercetin nanosuspensions fabricated by these three methods enhanced compared to the coarse quercetin.

1. Introduction

Nano-sized particles possess novel physiochemical properties which have been exploited for numerous applications in a variety of fields, especially in pharmaceutical and cosmetic industries. The key characteristic of drug nanocrystals is their enhanced ability to transport across a barrier such as cell membrane. This is why drug nanocrystals have been used for various application routes including parenteral [1], peroral [2], dermal [3,4], ocular [5], and pulmonary [6]. Nanocrystals also exhibit other advantages like increased saturation solubility and dissolution velocity attributed to their higher surface area, and excellent adhesion to biological surfaces [7]. This results in not only an improved bioavailability but also a reduction in variation in bioavailability of poorly soluble drugs, preferential class II drugs of the biopharmaceutical classification system (BCS) [8]. Therefore, there arises the need to find a simple yet efficient method to fabricate the drug nanocrystals that can be scaled up for use in the pharmaceutical industry. There are two key approaches to achieve the nano dimension namely, "top down" and "bottom up". The commonly used "top down" methods are high-pressure homogenization [9] and bead milling [10]. The main "bottom up" technique is precipitation. This "bottom up" precipitation method can be coupled with another "top down" method like homogenization to prevent the crystal growth of the precipitated nanocrystals into microcrystals. This precipitation–homogenization size reduction process called cavi-precipitation includes dissolving a drug in a good solvent, mixing the solvent with an antisolvent, and carrying out the precipitation in a zone of high energy to maintain the particle size achieved and to prevent further growth of the nanosuspension [11].

In the present study, quercetin has been used and its nanocrystals have been fabricated using the three methods viz., high-pressure homogenization, bead milling, and cavi-precipitation (H69, patent PCT/EP2006/009930). The three fabrication methods have been compared for the efficiency of production, the size and quality of the products obtained.

Quercetin has been used as a model drug. It is one of the most prominent dietary antioxidants and is claimed to exert beneficial health effects such as protection against osteoporosis, certain forms of cancer, pulmonary and cardiovascular diseases and also against aging [12]. However, quercetin presents a very low bioavailability (less than 17% in rats and even 1% in human) [13,14]. Apart from the considerable metabolism and high plasma protein binding in vivo (99.4%), its poor solubility leading to a very limited and slow absorption is also an important factor limiting the

* Corresponding author. School of Mechanical and Aerospace Engineering, Nanyang Technological University, 50 Nanyang Avenue, Singapore 639798, Singapore. Tel.: +65 6790 6285; fax: +65 6794 2035.
E-mail address: mlli@ntu.edu.sg (L. Li).

0939-6411/$ - see front matter © 2011 Elsevier B.V. All rights reserved.
doi:10.1016/j.ejpb.2011.08.006

bioavailability [15]. As a result, the clinical application of this drug is greatly restricted. Therefore, fabricating quercetin nanocrystals can greatly increase its saturation solubility and the dissolution velocity.

2. Methods and materials

2.1. Materials

Quercetin was purchased from Sigma Aldrich (Berlin, Germany). The stabilizer Tween 80 (polysorbate 80, Uniqema, Everberg, Belgium) was used for this study. Ultra purified water (Milli-Q, Millipore GmbH, Schwalbach/Ts., Germany) was used as the dispersion medium. All the reagents used were of technical grade.

2.2. Methods of preparation of nanosuspensions

2.2.1. High-pressure homogenization

Quercetin nanosuspensions of quercetin (5% and 10% w/w) in Milli-Q water with Tween 80 as stabilizer (1% and 2% w/w) were produced by high-pressure homogenization using LAB 40 (APV Deutschland GmbH, Unna, Germany) with a batch size of 40 ml. Firstly, the macrosuspensions were pre-milled at increasing pressures (2 cycles at 300 bar, 2 cycles at 500 bar, 1 cycle at 1000 bar) followed by high-pressure homogenization at 1500 bar for 20 homogenization cycles. For comparison, another set of samples was prepared at low homogenization pressure of 500 bar for 20 cycles. Samples for characterization were collected after pre-milling, and after 1, 5, 10, 15, and 20 cycles of homogenization.

2.2.2. Bead milling

Aqueous nanosuspensions of quercetin were fabricated using agitating bead mill Bühler PML-2 (Bühler AG, Uzwil, Switzerland) in a continuous mode. Yttrium-stabilized zirconia milling beads of size 0.4–0.6 mm and 0.2 mm were used as milling medium. The milling chamber (200 ml) was filled with 150 ml of milling medium and remaining with the coarse suspension of quercetin containing 5% and 10% (w/w) quercetin stabilized with Tween 80 (1% and 2% w/w). The milling was performed at a rotation speed of 2000 rpm for 90 min. The particle size of the milled quercetin suspension was assayed after 5, 30, 60, 90 min, and milling was stopped when an increase in particle size was observed.

2.2.3. Cavi-precipitation

Quercetin nanosuspensions were also prepared by the cavi-precipitation technique [16]. Quercetin solution was prepared in a suitable solvent like DMSO (20 ml) and ethanol (50 ml) and pumped at a fixed flow rate of 1 ml/min using an injection pump into the inflow reservoir of the Lab-Scale Microfluidiser HC-2000 (Microfluidics Inc., USA) containing the antisolvent (100 ml aqueous Tween 80 solution). Homogenization was performed at 500 bar. The nanosuspension was allowed to homogenize for another 10 min under 500 bar in continuous mode. The final nanosuspensions contained 5% and 0.5% (w/w) quercetin for the DMSO and ethanol formulations, respectively.

2.3. Particle size analyses

Photon correlation spectroscopy (PCS, Zetasizer Nano ZS, Malvern Instruments, UK) and laser diffractometry (LD, Coulter LS 230, Beckman-Coulter, Germany) were employed to determine the particle size of the quercetin nanosuspensions. PCS yields the mean particle size, and the polydispersity index (PDI) is a measure of the width of the size distribution. The PDI is 0.0 for a monodisperse particle population. PDI values of around 0.10–0.20 indicate a relatively narrow distribution, while PDI values of 0.5 and higher represent very broad distributions. The measurable range of the zetasizer is from approximately 0.6 nm to 6 μm. Thus, to observe larger particles, laser diffraction (LD) with a measuring range of up to 2000 μm was applied.

2.4. Particle morphology

Field emission scanning electron microscopy (FESEM, JEOL JSM-6700) was also used to analyze the morphology of the samples. The nanosuspensions were dropped onto a copper mesh, followed by drying under ambient conditions before measurement.

2.5. Zeta potential measurements

The zeta potential of the samples was measured by the Malvern zetasizer Nano ZS (Malvern Instruments, UK) in distilled water (conductivity = 50 μS/cm, pH 5.5–6) and in the original dispersion medium (the Tween 80 solution, pH 6.8) at 25 °C. The conductivity of distilled water was adjusted with 0.9% (w/v) sodium chloride solution. The mean value of the zeta potential and the standard deviation of three measurements were given.

2.6. X-ray diffraction (XRD)

In our XRD experiments, wide-angle X-ray scattering (WAXS) was used to assess the degree of crystallinity of the samples. XRD (or WAXS) patterns were generated using a Model PW 1830 Philips WAXS system (Philips Industrial & Electron-Acoustic Systems Division, Amedo, The Netherlands) equipped with a copper anode (Cu-Ka radiation, 40 kV, 25 mA l = 0.15418 nm) coupled with a Model PW18120 Goniometer detector. All measurements were recorded using a step width of 0.04°, a count time of 60 s, a 2θ scanning range, and speed set between 0.6–40° and 0.02° per second, respectively.

2.7. Solubility test

Solubility studies were performed in Milli-Q water with a shaker (InnovaTM 4230, New Brunswick Scientific Co., Inc., USA) at 25 °C, which allowed an accuracy of ±0.01 °C. Excess quercetin was added in 40 ml capped vials, which were sealed to avoid any changes due to evaporation and placed in a thermostated storage at 25 ± 0.01 °C for 1 week, shielded from light to prevent any degradation of the drug molecules. After the equilibrium was reached, suspensions were filtered through Sartorius® 0.1 μm filters (Sartorius AG, Germany). An aliquot from each vial was withdrawn by a 1 ml glass syringe (Poulten & Graf GmbH, Germany) and analyzed using HPLC. Experiments were carried out in triplicate, and solubility data were averaged.

2.8. Dissolution tests

The dissolution test was performed using a USP II rotating paddle apparatus with a Pharmatest PTW SIII (Pharma Test, Germany) at 37 °C and a rotating speed of 100 rpm in 900 ml of bidistilled water. Quercetin suspensions containing an equivalent of 5 mg of quercetin were dispersed in the dissolution medium. At certain desired times, samples were withdrawn from the dissolution chamber and filtered through Sartorius® 0.1 μm filters (Sartorius AG, Germany). An aliquot from each vial was withdrawn with a 1 ml glass syringe (Poulten & Graf GmbH, Germany) and analyzed using high performance liquid chromatography (HPLC). The dissolution test for each sample was performed in triplicate, and the dissolution data were averaged.

2.9. HPLC analysis of quercetin

Drug concentrations were determined by high performance liquid chromatography (HPLC). The chromatographic system consisted of a KromaSystem 2000 (Kontron Instruments GmbH, Germany), a solvent delivery pump equipped with a 20 μl loop and a rheodyne sample injector. Eurospere C18 (5 μm, 250 × 4 mm) analytical column was used, and the temperature was maintained at 37 °C. The mobile phase was composed of 25 mM potassium dihydrogen phosphate buffer and acetonitrile (50:50), and pH value was adjusted to 2.3 with hydrochloride acid. The flow rate was set at 0.5 ml/min, and an UV detector wavelength of 258 nm was used. The calibration curve of quercetin was linear (r^2 = 0.99) within the concentration range 1–50 μg/ml.

3. Results and discussion

3.1. Particle size study

3.1.1. High-pressure homogenization

The coarse quercetin microsuspension was subjected to pre-milling first to diminute very large crystals prior to the high-pressure homogenization in order to prevent blocking of the homogenization gap. The PCS diameter and polydispersity index (PDI) of quercetin nanocrystals fabricated at 500 bar and 1500 bar, as a function of homogenization cycles are shown in Fig. 1a. It was observed from Fig. 1a that the particle size decreased with increasing number of cycles. The number of homogenization cycles required is mainly influenced by the hardness of the drug, the finesse of the starting material, and the requirements of the application route or the final dosage form [9]. In case of quercetin nanocrystals, increasing the number of homogenization cycles from 15 to 20 did not reduce the particle size significantly. Therefore, 20 cycles were considered to be optimum for fabrication of quercetin nanosuspensions. It was also noted that increasing the homogenization pressure from 500 bar to 1500 bar reduced the crystal size to almost half. It has been shown previously that increasing the homogenization pressure does not promise a linear reduction in the crystal size [9]. During the homogenization process, the drug crystals mostly break at weak points or so-called crystal imperfections, which become lesser and lesser as the particle size decreases, meaning that the crystals become more and more perfect. Thus, the force required to break the crystals increases with decreasing particle size. If the force or homogenization pressure is equal to the attraction forces in the crystal, the crystal cannot be diminuted further, even when additional cycles of homogenization are applied, indicating that the smallest particle size at the given homogenization pressure is reached. From Fig. 1a, it was observed that the polydispersity index decreased initially and then fluctuated with the number of the homogenization cycles. These fluctuations in the PDI indicated slightly reversible aggregate formation during homogenization (increasing the PDI), where some aggregates were de-aggregated in the next cycles. Input of energy can also lead to aggregation as the energy, which is not utilized to diminute the particle size further, enhances the kinetic energy of the crystals, accelerates them and causes aggregation.

At both 500 and 1500 bar, two formulations with 5 wt% and 10 wt% quercetin were used to fabricate drug particles. The smallest average sizes obtained for the 5 wt% and 10 wt% formulations were 787.3 and 760.2 nm, respectively, at 500 bar, and 338.3 nm and 442 nm, respectively, at 1500 bar. The particle size distribution from laser diffractometry (LD) showed the unprocessed quercetin crystals with 50% and 95% of the particles smaller than 50.13 μm [$d(v)$50%] and 184.88 μm [$d(v)$95%], respectively. The $d(v)$95% values (LD data) for the 5 wt% and 10 wt% formulations fabricated at 1500 bar were 0.780 μm and 0.967 μm, respectively, indicating the absence of micron-sized particles. This is also confirmed by the FESEM microphotograph in Fig. 2b showing the 5 wt% quercetin nanosuspension homogenized for 20 cycles at 1500 bar. At the lower pressure (500 bar), a higher drug loading of quercetin (10 wt%) exhibited a smaller particle size because at a higher concentration, more particles absorbed the disintegration energy to increase collision of particles during the homogenization [17]. However, at a higher pressure (1500 bar), the trend was reversed and the formulation with 5 wt% quercetin gave a lower particle size. At 1500 bar, the power density applied was higher than that in the case of 500 bar, leading to greater reduction in particle size. Providing more energy led to aggregation of the particle in the case of 10 wt% formulation, and hence, it showed a larger particle size at 1500 bar.

3.1.2. Bead milling

Fig. 1b shows the particle size and polydispersity index of the drug nanocrystals prepared. For our study, yttrium-stabilized zirconia milling beads of two different size ranges, viz. 0.4–0.6 mm and 0.2 mm, were used as the milling medium. According to the theory, with a reduction in the size of milling media in a mill, the number of contact points is increased exponentially, resulting in improved grinding and dispersing action and hence leading to smaller sized particles. However, in our study, no major difference was observed in the particle size of the quercetin nanosuspensions fabricated using 0.2 mm and 0.4–0.6 mm sized milling beads. In fact, slightly higher particle size was obtained in the case of 0.2 mm sized milling beads. This indicates that decreasing the size of milling beads below a certain range does not necessarily lead to a decrease in the particle size. Moreover, it is easier to separate the 0.4–0.6 mm sized milling beads from the product than the 0.2 mm ones. Therefore, the 0.4–0.6 mm size milling beads were found to be efficient to obtain quercetin nanocrystals. Regarding the concentration of quercetin in the suspensions, no significant difference was observed in the particle size of the nanosuspensions containing 5 wt% and 10 wt% quercetin. When using 0.4–0.6 mm sized milling beads, 60 min were found to be sufficient to obtain the smallest average particle sizes of 253.2 nm and 270.7 nm for the 5 wt% and 10 wt% formulations, respectively. Bead milling for the next 30 min led to an increase in particle size to 319.6 and 276.6 nm, respectively. This is due to the fact that the additional input of energy does not lead to a further reduction in the particle size, but enhances the kinetic energy of the crystals, causing aggregation. The similar observation was made using 0.2 mm milling beads, where milling was stopped after 60 min, and the average particle sizes of 340.2 nm and 337.3 nm were obtained for the 5 wt% and 10 wt% formulations, respectively. The $d(v)$95% (LD data) for both 5 wt% and 10 wt% formulations indicated that no particles bigger than 0.801 μm and 0.728 μm were present in the corresponding quercetin nanosuspensions. It can also be inferred from the FESEM microphotograph of the 5 wt% bead milled quercetin (0.4–0.6 mm beads) in Fig. 2c that there were no aggregations.

The bead milled (using 0.4–0.6 mm size beads) samples exhibiting the smallest particle size for both 5 wt% and 10 wt% formulations were further treated with high-pressure homogenization at 1500 bar to investigate if the particle size could be reduced further. For the 10 wt% formulation, after homogenizing for three cycles at 1500 bar, the average particle size decreased slightly to 249.5 nm from 276.7 nm and PDI changed to 0.123 from 0.121. Homogenizing for more cycles did not decrease the particle size further. Unfortunately, for the 5 wt% formulation, the particle size did not decrease after homogenizing at 1500 bar, but the PDI decreased from 0.129 to 0.122. We found that the smallest crystal size that can be obtained for quercetin by "top down" techniques is approximately 250 nm.

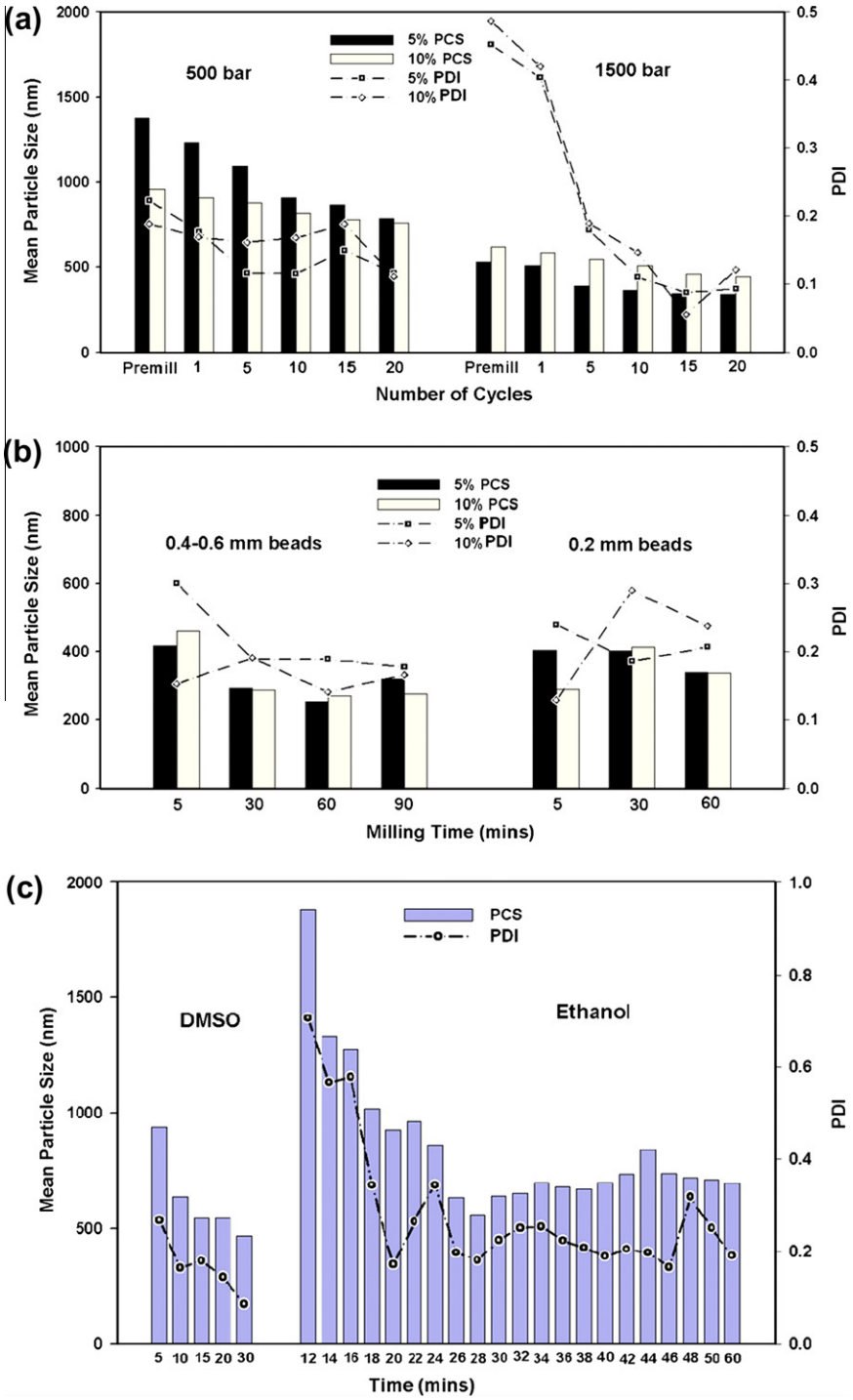

Fig. 1. Particle diameter (PCS) and polydispersity index (PDI) as a function of (a) homogenization cycle for quercetin nanosuspensions produced by high-pressure homogenization at 500 bar and 1500 bar, (b) milling time for quercetin nanosuspensions produced by bead milling using 0.2 mm and 0.4–0.6 mm sized milling beads, and (c) time for quercetin nanosuspensions produced by cavi-precipitation using different solvents (DMSO and ethanol). (For interpretation of the references to color in this figure legend, the reader is referred to the web version of this article.)

3.1.3. Cavi-precipitation

The main challenge associated with precipitation is to stop the growth of crystals. This can be done by carrying out precipitation in a high energy zone, i.e., in a microfluidizer [11]. In cavi-precipitation, precipitation is accompanied by homogenization at 500 bar. For the precipitation process, quercetin was dissolved in DMSO and pumped at a rate of 1 ml/min. The smallest average particle size obtained was 469.7 nm with a PDI of 0.111 as seen from Fig. 1c and the FESEM microphotograph in Fig. 2d. However, since the safety of DMSO in pharmaceuticals is questionable due to its toxic side effect [18], an additional step has to been taken to remove DMSO. Therefore, ethanol was used instead of DMSO, as ethanol can be used in the final formulation as well. As the solubility of quercetin in ethanol is comparatively lower, a lower concentration of quercetin was obtained. The lowest average particle size of 559.4 nm and PDI of 0.180 were obtained after 28 min as

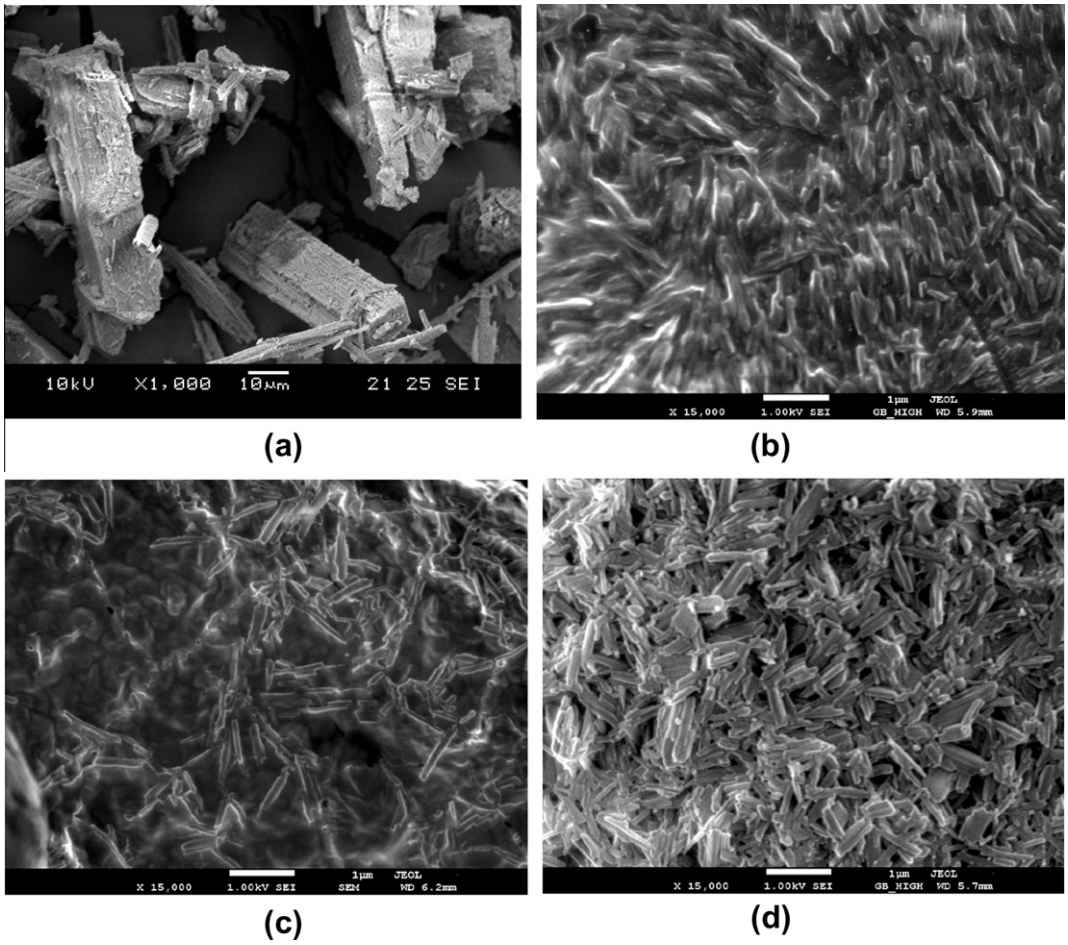

Fig. 2. FESEM microphotographs of (a) coarse quercetin; and the nanosuspensions of quercetin produced by (b) high-pressure homogenization ($H5_{1500}$), (c) bead milling ($M5_{0.4-0.6}$), and (d) cavi-precipitation ($C5_{DMSO}$).

observed from Fig. 1c. However, the average particle size and PDI were 694.9 nm and 0.191, respectively, after 60 min when the entire quercetin solution in ethanol had been pumped. There were fluctuations in the average particle size and PDI with time due to two overlapping phenomena occurring simultaneously. One was the breaking of drug crystals due to homogenization and the other was the simultaneous precipitation of the new drug crystals along with the growth of the existing ones. These two opposite processes of reducing the particle size and increasing the particle size occurring concurrently led to the fluctuations in the measured particle size and PDI values. It is very difficult to predict which of the two phenomena was dominant at a particular time. The $d(v)95\%$ (LD data) for both formulations with DMSO and ethanol indicated that no particles bigger than 0.843 μm and 1.112 μm were present in the corresponding nanosuspensions. Another experiment was conducted to test the influence of pumping rate of the quercetin solution into the antisolvent. A flow rate of 0.25 ml/min was used to pump the quercetin solution into ethanol. The lowest particle size obtained was 484.1 and PDI was 0.146. Although the particle size decreased after decreasing the pumping rate but the production time increased 4 times. To conclude, the decrease in the particle size is not significant after increasing the production time by fourfold.

3.2. Zeta potential

The zeta potential was measured in distilled water and the original media of the nanosuspensions. Zeta potentials above the absolute value of 30 mV are required for a storage stability of a charge-stabilized dispersion [19]. Table 2 gives the zeta potential values of different samples in water and Tween 80 solution. The zeta potential of all the formulations in distilled water was around −30 mV or less. However, the zeta potential values in the original dispersion media (Tween 80 solution) for all the nanosuspensions were around −20 mV (lower for the cavi-precipitated nanosuspensions). A thicker adsorption layer of Tween 80, led to a shift of the plane of shear to a larger distance from the particle surface, and thus, to a reduction in the measured potential. The employed stabilizer (Tween 80) acts as a steric stabilizer due to its nonionic structure, and nanosuspensions can be stable even without any electrostatic contribution from Tween 80. It should be noted that adsorption of a steric stabilizer layer led to a reduction in the measured zeta potential, but it is not an indication of a reduced stability. In such cases, zeta potentials of about 20 mV are still sufficient to stabilize the system in combination with steric stabilization [20].

The zeta potential of the quercetin nanosuspensions in distilled water was in the following order: milled > homogenized > cavi-precipitated. The values of zeta potential of the quercetin nanosuspensions in Tween 80 solution were quite low due to the steric stabilization as explained above and exhibited the same trend as the zeta potential values in the distilled water. From the zeta potential values in Table 2, it was seen that the nanocrystals fabricated by cavi-precipitation showed very low zeta potential values, and hence, their stability was predicted to be low. This might be attributed to the presence of the solvent residues in the

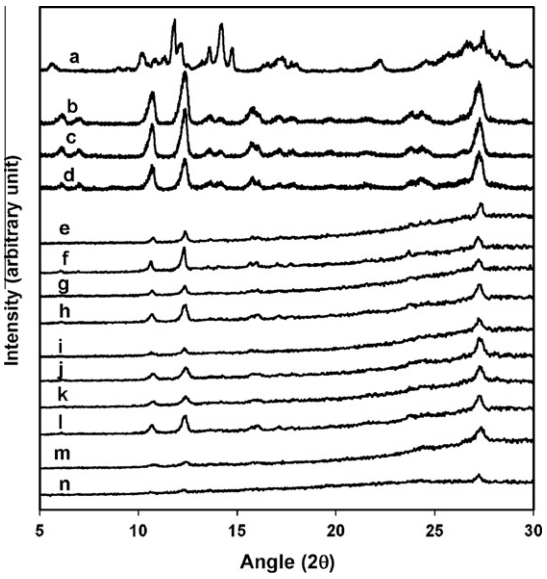

Fig. 3. X-ray diffractogram of (a) coarse quercetin powder; dried quercetin nanosuspension samples: (b) $H5_{1500}$, (c) $M5_{0.4–0.6}$, and (d) $C5_{DMSO}$; and (e)–(n) quercetin nanosuspensions in the order as samples 1–10 listed in Table 2.

nanosuspensions. Approximately 16% (20 ml in 94 ml water) of DMSO and 33.5 wt% (50 ml in 99.4 ml water) of ethanol were present in the final product. The surfactant and the solvent competed for water for hydration, which decreased the stability of the final product.

3.3. Powder X-ray diffraction

The extent of crystallinity also influences the solubility and dissolution rate of a drug, and hence, the product performance and effectiveness. An amorphous or metastable form dissolves at a faster rate because of its higher internal energy and greater molecular mobility compared to crystalline materials [21]. However, the major challenge is the stability of the amorphous state during a shelf life of the product. The amorphous state needs to be maintained during the shelf life of a product to avoid a decrease in oral bioavailability [22]. In general, more crystalline substances are physically more stable than the amorphous forms. The X-ray diffraction (XRD) patterns for all the samples are presented in Fig. 3. The X-ray patterns of the quercetin powder in Fig. 3a displayed the presence of numerous distinct peaks at 2θ of 5.54°, 10.22°, 11.82°, 14.18°, 17.24°, 22.16°,and 27.48°, which suggests that the drug was of a crystalline form. In the case of dried quercetin nanocrystals in Fig. 3b–d, some peaks shifted slightly to the higher side but peak intensities were similar, suggesting the crystalline nature of the quercetin nanocrystals fabricated by different methods. For the quercetin nanocrystals in the nanosuspensions produced, the XRD patterns in Fig. 3e–n indicated that all nanocrystals were still in the crystalline state after being fabricated by the three methods. The quercetin nanocrystals showed the diffraction peaks with lower intensities due to the presence of only 0.5 wt% or 5 wt% or 10 wt% quercetin in the nanosuspensions as described in Table 1. Applying energy by high-pressure homogenization, milling or cavi-precipitation did not transform quercetin into an amorphous state. It has also been previously reported that the crystalline state of the drug was same after high-pressure homogenization [23].

3.4. Solubility study

Table 2 shows the saturation solubility measured for the coarse quercetin and its nanocrystals fabricated by the three methods. The saturation solubility of coarse quercetin was extremely low being only 2.84 ± 0.03 μg/ml. There was the significant enhancement in the saturation solubility of the nanocrystals produced by

Table 1
Fabrication method, fabrication condition, sample composition, average particle size measured by PCS and polydispersity index (PDI) for various samples prepared.

Method	Condition	Sample name	Composition (%, w/w)			PCS (nm)	PDI
			Quercetin	Tween 80	Water		
HPH	500 bar	$H5_{500}$	5	1	94	787.3	0.116
		$H10_{500}$	10	2	88	760.2	0.111
	1500 bar	$H5_{1500}$	5	1	94	338.3	0.093
		$H10_{1500}$	10	2	88	442.0	0.121
Bead milling	0.4–0.6 mm beads	$M5_{0.4–0.6}$	5	1	94	319.6	0.129
		$M10_{0.4–0.6}$	10	2	88	276.7	0.121
	0.2 mm beads	$M5_{0.2}$	5	1	94	340.2	0.207
		$M10_{0.2}$	10	2	88	337.3	0.238
Cavi-precipitation	DMSO (20 ml)	$C5_{DMSO}$	5	1	94	469.7	0.111
	Ethanol (50 ml)	$C0.5_{Ethanol}$	0.5	0.1	99.4	694.9	0.191

Table 2
The $d(v)50\%$, $d(v)95\%$, and zeta potential values of all the samples in water and a Tween 80 solution, along with their saturation solubility.

	Sample name	$d(v)50\%$ (in μm)	$d(v)95\%$ (in μm)	Zeta potential (mV)		Saturation solubility (μg/ml)
				Distilled water	Tween 80 solution	
1	$H5_{500}$	0.798	1.556	−25.3 ± 1.37	−19.91 ± 0.04	13.80 ± 0.92
2	$H10_{500}$	0.765	1.367	−24.8 ± 0.64	−20.09 ± 0.12	13.27 ± 1.32
3	$H5_{1500}$	0.373	0.780	−28.4 ± 1.15	−19.7 ± 0.92	22.74 ± 0.77
4	$H10_{1500}$	0.457	0.967	−27.3 ± 0.11	−18.8 ± 1.67	20.26 ± 0.81
5	$M5_{0.4–0.6}$	0.325	0.801	−30.5 ± 0.02	−20.2 ± 0.90	24.06 ± 0.90
6	$M10_{0.4–0.6}$	0.280	0.728	−31.7 ± 1.61	−21.5 ± 0.09	25.59 ± 1.11
7	$M5_{0.2}$	0.363	0.824	−29.2 ± 0.78	−20.24 ± 0.90	22.26 ± 0.69
8	$M10_{0.2}$	0.346	0.816	−32.2 ± 0.72	−22.93 ± 0.04	23.15 ± 1.05
9	$C5_{DMSO}$	0.470	0.843	−19.3 ± 0.51	−11.5 ± 0.53	18.26 ± 1.94
10	$C0.5_{Ethanol}$	0.707	1.112	−18.3 ± 0.29	−10.1 ± 0.63	41.36 ± 1.78
11	Coarse quercetin	174.39	184.88	–	–	2.84 ± 0.03

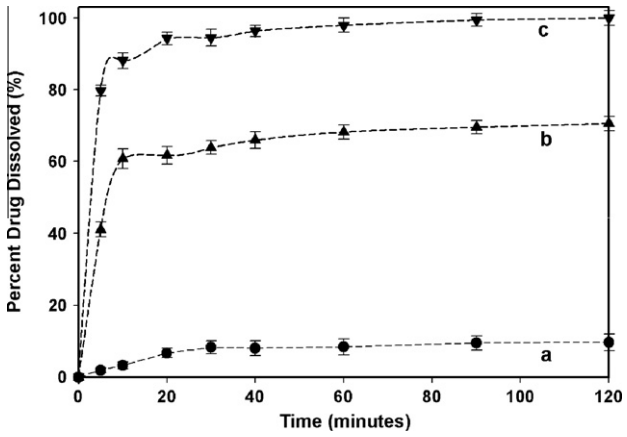

Fig. 4. Dissolution profiles of (a) coarse quercetin microsuspension, (b) $H5_{500}$, nanosuspension homogenized at 500 bar, and (c) $M5_{0.4-0.6}$, bead milled nanosuspension.

the three methods. This is because the saturation solubility increases with decreasing particle size below 1000 nm [9]. Forming nanocrystals enhanced the saturation solubility of quercetin approximately nine times to 25.59 ± 1.11 μg/ml for the milled (0.4–0.6 mm sized beads) nanosuspension containing 10 wt% quercetin. However, it was surprising to note the exceptionally high saturation solubility values of 18.26 ± 1.94 μg/ml and 41.36 ± 1.78 μg/ml for the cavi-precipitated products using DMSO and ethanol as a solvent, respectively, as their particle sizes were larger. The higher saturation solubility values were due to the presence of the solvents in the final product. From these results, the cavi-precipitated nanosuspension using ethanol as the solvent exhibited the highest solubility and can be suitable for use in the final formulations.

The solubility studies were performed in Milli-Q water and samples were taken every 24 h. The saturation solubility did not decrease significantly and remained almost the same for seven days. Usually, the presence of micrometer-sized crystals (acting as nuclei for crystallization) causes the concentration to decrease by re-crystallization (growth of microcrystals being present). Therefore, it is important to have no or little microcrystals in a nanosuspension. In the quercetin nanocrystal formulations prepared, the microcrystals were absent or present in limited amount, and hence, the saturation solubility remained unchanged. Besides that, after saturation, the amorphous form may recrystallize into the crystalline form. However, as there were no amorphous fractions of quercetin in the formulations prepared as known by DSC thermogram and X-ray diffractogram, the saturation solubility did not decrease after seven days. This is favorable for oral administration. Some nanocrystals show a low bioavailability because they dissolve in the gut, but immediately recrystallize into large microcrystals. Thus, the real concentration of the drug and subsequently its bioavailability decreases.

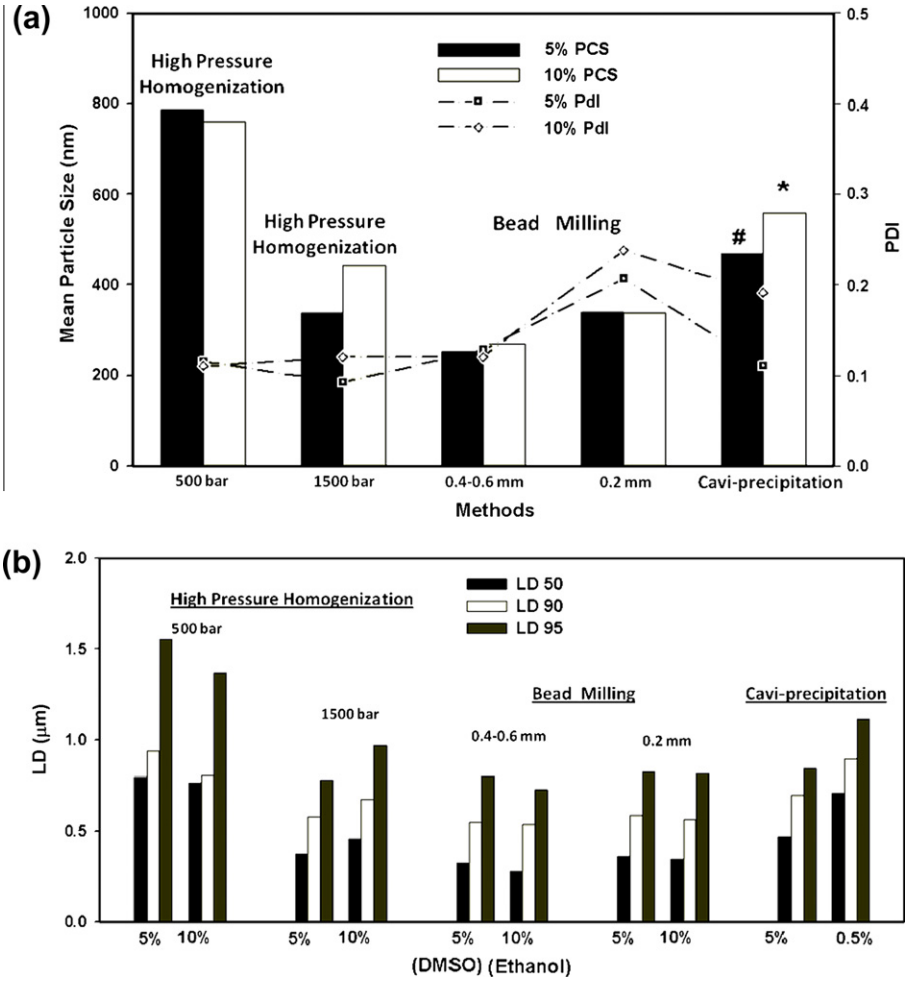

Fig. 5. Comparison of (a) average PCS particle size and polydispersity index [# – nanosuspension containing 5 wt% quercetin and DMSO as solvent, * – nanosuspension containing 0.5 wt% quercetin and ethanol as solvent], and (b) particle size distributions (LD data) of the nanosuspensions produced by all the three methods.

3.5. Dissolution study

Dissolution test was performed for the coarse quercetin and the milled nanosuspension (0.4–0.6 mm sized beads) containing 10 wt% quercetin, which showed the lowest particle size. One more sample with intermediate particle size, the homogenized nanosuspension (500 bar) containing 10 wt% quercetin, was also chosen to compare the dissolution rate. As seen from the dissolution profile in Fig. 4, only about 10% of the coarse quercetin dissolved within 120 min as compared to 100% for the bead milled nanosuspension. The nanosuspension homogenized at 500 bar exhibited 70% dissolution within 120 min. These results can be explained by the Noyes–Whitney equation [24], according to which, the dissolution rate of a drug can be increased by reducing the particle size to increase the particles surface area. Besides that, nanosizing the drug also leads to enhanced saturation solubility as described above, which again contributes to a higher dissolution velocity. Therefore, nanosizing quercetin tremendously increased enhanced its dissolution rate.

3.6. Comparison of fabrication methods

Looking at the average PCS particle size in Fig. 5, bead milling produced the lowest particle size, followed by high-pressure homogenization and then cavi-precipitation. Examining the corresponding LD data, it was observed that there were no significant differences among the various nanosuspensions except the one fabricated by homogenization at 500 bar. Comparison of the three methods of fabrication showed that each technique had its own advantages and disadvantages. Bead milling with 0.4–0.6 mm sized beads resulted in the smallest particle size. High-pressure homogenization at 1500 bar produced slightly larger nanocrystals but the polydispersity index was lower than that of the bead milled product. The zeta potential of the two products was also comparable as seen from Table 2. Therefore, considering the particle size, the polydispersity index and the zeta potential, not much difference was noted between bead milling and high-pressure homogenization. Bead milling has certain disadvantages like potential erosion from the milling material leading to product contamination, potential growth of germs in the water phase when milling for a long time, and time and costs associated with the separation procedure of the milling material from the drug nanosuspensions [25]. For producing quercetin nanosuspension, 60 min were found to be sufficient and the short milling time is expected to minimize the above-mentioned side effects and hence ensure good quality of the product. However, the separation of the milling media from the nanosuspension is still a problem. For high-pressure homogenization, 20 cycles at 1500 bar were used to fabricate the drug nanosuspension, but the application of such high pressures can affect the large-scale pharmaceutical production. To sum up, bead milling and high-pressure homogenization both presented an efficient means to fabricate stable quercetin nanosuspensions. It was also observed that homogenizing the bead milled product led to a smaller particle size and a lower polydispersity index. The zeta potential values of bead milled and homogenized nanosuspensions in distilled water were ~ -32 mV, and ~ -27.47 mV Tween 80 solution, indicating good stability. Therefore, both methods are shown to be suitable. Cavi-precipitation is comparatively a low energy and simple process, and processing parameters can be altered to achieve the desired product. Although the cavi-precipitated product was not stable as indicated by the zeta potential values, but the cavi-precipitated quercetin nanosuspension with ethanol showed the highest solubility. The problem with solvent residue can be overcome by using nontoxic solvents like ethanol, and further dilution of the final product can eliminate the stability problem. With regard to a potential dermal application of quercetin nanosuspensions, incorporation into a hydrogel would be a promising approach to increase the physical stability. Therefore, increasing the viscosity of the aqueous phase of nanosuspensions can improve physical stability by reducing particle mobility and hence preventing agglomeration of quercetin nanocrystals.

4. Conclusions

Quercetin nanocrystals were successfully fabricated by means of three methods, namely high-pressure homogenization, bead milling and cavi-precipitation. The smallest particles of around 276.7 nm were obtained by bead milling product and they demonstrated a saturation solubility of 25.59 ± 1.11 μg/ml, about nine times higher than coarse quercetin. Bead milling fabricated the smallest particle size whereas high-pressure homogenization gave the lowest polydispersity index. The cavi-precipitated product exhibited the larger particle size but it showed a higher saturation solubility due to the presence of ethanol. The zeta potential indicated a good stability for all the products except for the cavi-precipitated product. The quercetin nanocrystals dissolved much faster than the coarse quercetin.

Acknowledgments

The authors acknowledge the support of Deutscher Akademischer Austauschdienst—DAAD (PKZ: A/09/74578). The work was supported also by the Lee Kuan Yew Fellowship and SUG Grant M58050023, Nanyang Technological University, Singapore.

References

[1] R.H.H. Neubert, Potentials of new nanocarriers for dermal and transdermal drug delivery, Eur. J. Pharm. Biopharm. 77 (2011) 1–2.
[2] A.M. Cerdeira, M. Mazzotti, B. Gander, Miconazole nanosuspensions: influence of formulation variables on particle size reduction and physical stability, Int. J. Pharm. 396 (2010) 210–218.
[3] A.O.K. Hassan, A.H. Elshafeey, Nanosized particulate systems for dermal and transdermal delivery, J. Biomed. Nanotechnol. 6 (2010) 621–633.
[4] A. Schroeter, T. Engelbrecht, R.H.H. Neubert, A.S.B. Goebel, New nanosized technologies for dermal and transdermal drug delivery. A review, J. Biomed. Nanotechnol. 6 (2010) 511–528.
[5] M.A. Kassem, A.A.A. Rahman, M.M. Ghorab, M.B. Ahmed, R.M. Khalil, Nanosuspension as an ophthalmic delivery system for certain glucocorticoid drugs, Int. J. Pharm. 340 (2007) 126–133.
[6] W.H. Roa, S. Azarmi, M.H.D.K. Al-Hallak, W.H. Finlay, A.M. Magliocco, R. Löbenberg, Inhalable nanoparticles, a non-invasive approach to treat lung cancer in a mouse model, J. Control. Release 150 (2011) 49–55.
[7] R.B. Gupta, Fundamentals of drug nanoparticles, in: R.B. Gupta, U.B. Kompella (Eds.), Nanoparticle Technology for Drug Delivery, Taylor & Francis, New York, 2006, pp. 3–4.
[8] G.L. Amidon, H. Lennernas, V.P. Shah, J.R. Crison, A theoretical basis for a biopharmaceutic drug classification: the correlation of in vitro drug product dissolution and in vivo bioavailability, Pharm. Res. 12 (1995) 413–420.
[9] C.M. Keck, R.H. Müller, Drug nanocrystals of poorly soluble drugs produced by high pressure homogenization, Eur. J. Pharm. Biopharm. 62 (2006) 3–16.
[10] G.G. Liversidge, K.C. Cundy, J.F. Bishop, D.A. Czekai, US Patent 145,684, 1992.
[11] R.H. Müller, J. Moschwitzer, Method and device for producing very fine particles and coating such particles, Patent PCT/EP2006/009930, 2006.
[12] A.W. Boots, G.R. Haenen, A. Bast, Health effects of quercetin: from antioxidant to nutraceutical, Eur. J. Pharmacol. 585 (2008) 325–337.
[13] M.M. Chan, D. Fong, K.J. Soprano, W.F. Holmes, H. Heverling, Inhibition of growth and sensitization to cisplatin-mediated killing of ovarian cancer cells by polyphenolic chemopreventive agents, J. Cell. Physiol. 194 (2003) 63–70.
[14] K.A. Khaled, Y.M. El-Sayed, B.M. Al-Hadiya, Disposition of the flavonoid quercetin in rats after single intravenous and oral doses, Drug Dev. Ind. Pharm. 29 (2003) 397–403.
[15] V.A. Bhattaram, U. Graefe, C. Kohlert, M. Veit, H. Derendorf, Pharmacokinetics and bioavailability of herbal medicinal products, Phytomedicine 9 (2002) 1–33.
[16] M. Kakran, R. Shegokar, L. Al Shaal, N.G. Sahoo, L. Li, R.H. Müller, Production Optimization of Antioxidant Quercetin Nanocrystals, Abstract 2265, AAPS Annual Meeting and Exposition, October 23–27, 2011, Washington, DC, USA.
[17] K. Krause, R.H. Müller, Production and characterisation of highly concentrated nanosuspensions by high pressure homogenization, Int. J. Pharm. 214 (2001) 21–24.

[18] P. Ader, A. Wessmann, S. Wolffram, Bioavailability and metabolism of the flavonol quercetin in the pig, Free Radic. Biol. Med. 28 (2000) 1056–1067.
[19] R.M. Mainardes, R.C. Evangelista, PLGA nanoparticles containing praziquantel: effect of formulation variables on size distribution, Int. J. Pharm. 290 (2005) 137–144.
[20] D.S. Kohane, J.Y. Tse, Y. Yeo, R. Padera, M. Shubina, L. Robert, Biodegradable polymeric microspheres and nanospheres for drug delivery in the peritoneum, J. Biomed. Mater. Res. Part A 77A (2006) 351–361.
[21] M. Kakran, N.G. Sahoo, L. Li, Z. Judeh, Y. Wang, K. Chong, L. Loh, Fabrication of drug nanoparticles by evaporative precipitation of nanosuspension, Int. J. Pharm. 383 (2010) 285–292.
[22] M. Thommes, D.R. Ely, M.T. Carvajal, R. Pinal, Improvement of the dissolution rate of poorly soluble drugs by solid crystal suspensions, Mol. Pharm. 8 (2011) 727–735.
[23] R. Mauludin, R.H. Müller, C.M. Keck, Kinetic solubility and dissolution velocity of rutin nanocrystals, Eur. J. Pharm. Sci. 36 (2009) 502–510.
[24] A.A. Noyes, W.R. Whitney, The rate of solution of solid substances in their own solutions, J. Am. Chem. Soc. 19 (1897) 930–934.
[25] R.H. Müller, A. Akkar, Drug nanocrystals of poorly soluble drugs, in: H.S. Nalwa (Ed.), Encyclopedia of Nanoscience and Nanotechnology, American Scientific Publishers, 2004, pp. 627–638.